Developmental and Comparative Immunology 52 (2015) 48–57

Contents lists available at ScienceDirect

Developmental and Comparative Immunology

journal homepage: www.elsevier.com/locate/dci

Molecular cloning, expression and functional characterization of a teleostan cytokine-induced apoptosis inhibitor from rock bream (*Oplegnathus fasciatus*)

Don Anushka Sandaruwan Elvitigala [a,b], H.K.A. Premachandra [a], Ilson Whang [a,b,*], Sang-Yeob Yeo [c], Cheol Young Choi [d], Jae Koo Noh [e], Jehee Lee [a,b,**]

[a] Department of Marine Life Sciences, School of Marine Biomedical Sciences, Jeju National University, Jeju Self-Governing Province 690-756, Republic of Korea
[b] Fish Vaccine Development Center, Jeju National University, Jeju Special Self-Governing Province 690-756, Republic of Korea
[c] Department of Biotechnology, Division of Applied Chemistry & Biotechnology, Hanbat National University, Daejeon 305-719, Republic of Korea
[d] Division of Marine Environment & Bioscience, Korea Maritime University, Busan 606-791, Republic of Korea
[e] Genetics & Breeding Research Center, National Fisheries Research & Development Institute, Geoje 656-842, Republic of Korea

ARTICLE INFO

Article history:
Received 14 November 2014
Revised 26 March 2015
Accepted 28 March 2015
Available online 23 April 2015

Keywords:
Cytokine-induced apoptosis inhibitor
Rock bream
Transcriptional analysis
Genomic gene structure
Caspase inhibitory activity

ABSTRACT

Apoptosis plays a key role in the physiology of multicellular organisms and is regulated by different promoting and inhibitory mechanisms. Cytokine-induced apoptotic inhibitor (CIAPI) was recently identified as a key factor involved in apoptosis inhibition in higher vertebrate lineages. However, most of the CIAPIs of lower vertebrate species are yet to be characterized. Herein, we molecularly characterized a teleostan counterpart of CIAPI from rock bream (*Oplegnathus fasciatus*), designating as RbCIAPI. The complete coding region of *RbCIAPI* was consisted of 942 nucleotides encoding a protein of 313 amino acids with a predicted molecular mass of ~33 kDa. RbCIAPI gene exhibited a multi-exonic architecture, consisting 9 exons interrupted by 8 introns. Protein sequence analysis revealed that RbCIAPI shares significant homology with known CIAPI counterparts, and phylogenetic reconstruction confirmed its closer evolutionary relationship with its fish counterparts. Ubiquitous spatial distribution of RbCIAPI was detected in our quantitative real time polymerase chain reaction (qPCR) analysis, where more prominent expression levels were observed in the blood and liver tissues. Moreover, the *RbCIAPI* basal transcription level was found to be modulated by different bacterial and viral stimuli, which could be plausibly supported by our previous observations on the transcriptional modulation of the caspase 3 counterpart of rock bream (Rbcasp3) in response to the same stimuli. In addition, our *in vitro* functional assay demonstrated that recombinant RbCIAPI could detectably inhibit the proteolysis activity of recombinant Rbcasp3. Collectively, our preliminary results suggest that RbCIAPI may play an anti-apoptotic role in rock bream physiology, likely by inhibiting the caspase-dependent apoptosis pathway. Therefore, RbCIAPI potentially plays an important role in host immunity by regulating the apoptosis process under pathogenic stress.

1. Introduction

Development of a multicellular organism highly depends on the equilibrium between cell proliferation and cell death; processes that are tightly regulated by different mechanisms including programmed cell death (PCD) (Danial and Korsmeyer, 2004). Apoptosis is a type of PCD, and is considered as a key component of the development and aging processes, as well as a homeostatic mechanism to maintain cell populations in tissues (Elmore, 2007). Moreover, apoptosis is known to be induced as a host defense mechanism through mediating immune responses, especially immune responses mounted against viral infections (Everett and McFadden, 1999; Sun and Shi, 2001), and counterbalance the consequences of pathological conditions. However, proper regulation of apoptosis, in terms of its activation and inhibition, is also required to maintain a proper life cycle. In this regard, BCl-2 family proteins are known to be prominent players in pro-apoptotic and anti-apoptotic processes (Burlacu, 2003), whereas inhibitor of apoptosis proteins (IAPs) are widely known to obstruct the apoptotic process (Deveraux and Reed, 1999).

* Corresponding author. Marine Molecular Genetics Lab, Department of Marine Life Sciences, College of Ocean Science, Jeju National University, 66 Jejudaehakno, Ara-Dong, Jeju 690-756 Korea. Tel.: +82 64 754 3472; fax: +82 64 756 3493.
E-mail address: ilsonwhang@hanmail.net (I. Whang).
** Corresponding author. Marine Molecular Genetics Lab, Department of Marine Life Sciences, College of Ocean Science, Jeju National University, 66 Jejudaehakno, Ara-Dong, Jeju 690-756, Republic of Korea. Tel.: +82 64 754 3472; fax: +82 64 756 3493.
E-mail address: jehee@jejunu.ac.kr (J. Lee).

http://dx.doi.org/10.1016/j.dci.2015.03.016
0145-305X/

Besides the prominent modulators of apoptosis mentioned earlier, another potent inhibitor of apoptosis, designated as cytokine-induced apoptosis inhibitor (CIAPI) or anamorsin has been identified from mice as an essential component of definitive hematopoiesis (Shibayama et al., 2004). CIAPI deficiency was found to induce significant apoptosis in hematopoietic cells in fetal livers of mice, which was accompanied by downregulated expression levels of Bcl-xL and Jak2, suggesting CIAPI as a potential candidate for inducing Bcl-xL and Jak2 expression.

CIAPI exhibits an extensive spatial distribution in both fetal and adult tissues of animals. For instance, more pronounced expression levels of CIAPI were observed in various regions of the rat central nervous system including the cerebral cortex, hippocampus, midbrain, cerebellum medulla, and spinal cord (Park et al., 2011). Moreover, cytosolic CIAPI in rats could be translocated into the nucleus upon reactive oxygen species (ROS) production, and is potentially involved in the regulation of transcription of vital proteins that are important in dopaminergic neurodegeneration (Park et al., 2011). A recent report showed that CIAPI of the well-known human parasite *Schistosoma japonicum* (schistosoma) could inhibit the caspase activity induced by cytokines such as interleukin-β and tumor necrosis factor-α in either human cell lines or schistosome lysates, and it could therefore be considered as a potential drug target against schistosomiasis (Luo et al., 2012).

Abundant expression of CIAPI was observed under some neoplastic conditions in different types of cancer cells including hepatocellular carcinoma, gastric cancer, leukemia and B-cell lymphoma cells, and was associated with clinicopathological characteristics of tumor aggressiveness. This observation further supports the candidature of CIAPI as a prognostic marker of cancer in humans (Gastric and Cells, 2006; Li et al., 2007, 2008; Shizusawa et al., 2008). Moreover, another study showed that the multidrug resistance (MDR) of human gastric cancer cells could be triggered by CIAPI through up-regulating MDR1 at the transcriptional and translational levels (Gastric and Cells, 2006), demonstrating the mediatory properties of CIAPI on gastric cancer MDR. However, the exact physiological function of CIAPI is yet to be elucidated in animals.

Although information on CIAPI of higher vertebrates, such as mice and humans, is currently available, characterization studies on CIAPI of lower vertebrates, especially from fish, are lacking.

Edible marine fish are considered as a protein-rich resource in human diets; thus, mariculture farming of fish has been widely adopted to compensate for the increasing demand. However, as a consequence of intensive, large-scale culturing of fish in restricted areas, different stress factors, particularly pathogenic stress, have adversely affected the yield of fish mariculture farming worldwide, resulting in considerable economic loss. Considering this background, investigations on the molecular mechanism underlying the pathophysiology of mariculture fish species can be considered as a preliminary step toward developing disease management strategies to combat the growing threat of pathogenic infections on farmed fish populations.

Herein, we attempted to characterize a teleostan counterpart of CIAPI, identified from rock bream (*Oplegnathus fasciatus*), as the first such characterization report from fish, evaluated its transcriptional modulation under pathogenic stress, and further demonstrated its potent inhibitory properties against the previously identified ortholog of caspase 3 from the same species.

2. Materials and methods

2.1. Identification and sequence characterization of rock bream *CIAPI* (RbCIAPI)

Analysis of our previously established cDNA sequence database using the Basic Local Alignment Search Tool (BLAST) algorithm (http://blast.ncbi.nlm.nih.gov/Blast.cgi) led to the identification of the complete cDNA sequence of *RbCIAPI*, which was analyzed and compared with its orthologs using bioinformatics. The complete coding region of *RbCIAPI* and its corresponding amino acid sequence were derived using DNAsist 2.2 software, and the domains of the protein were predicted using the SMART online server (http://smart.embl-heidelberg.de/). Some of the physicochemical properties of RbCIAPI were determined using the ExPASy ProtParam tool (http://web.expasy.org/protparam). The derived protein sequence of RbCIAPI was compared with its orthologs through pairwise sequence alignments and multiple sequence alignment using the EMBOSS Needle (http://www.Ebi.ac.uk/Tools/emboss/align) and ClustalW2 (http://www.Ebi.ac.uk/Tools/clustalw2) programs, respectively. The evolutionary relationship of RbCIAPI with other vertebrate as well as invertebrate counterparts at the molecular level was determined using phylogenetic analysis using Molecular Evolutionary Genetics Analysis (MEGA) software version 4 (Tamura et al., 2007), following the neighbor-joining method, supported by 1000 bootstrapped replications.

In addition, we identified the complete genomic sequence of *RbCIAPI* using our custom-constructed random sheared rock bream BAC genomic DNA (gDNA) library (Lucigen®; USA). The BAC clone containing the genomic *RbCIAPI* gene was analyzed using a two-step polymerase chain reaction (PCR)-based screening approach of our gDNA library with a gene-specific primer pair (RbCIAPI_qF and RbCIAPI_qR; Table 1) according to the manufacturer's instructions. After localizing the putative clone bearing gDNA of *RbCIAPI*, it was sequenced by GS-FLX™ system (Macrogen, Korea), and the complete genomic sequence of *RbCIAPI* was obtained. Thereafter, the obtained gDNA sequence was compared with the previously identified complete cDNA sequence using the National Center for Biotechnology Information (NCBI) 'Spidey' online server (http://www.ncbi.nlm.nih.gov/spidey) to obtain the annotation of exon–intron arrangement.

2.2. Cloning, over expression, and purification of recombinant RbCIAPI (*rRbCIAPI*)

Recombinant RbCIAPI was expressed as a fusion protein with maltose binding protein (MBP), and purified as described in the pMAL protein fusion and purification protocol (New England BioLabs, USA). Briefly, the complete coding sequence of *RbCIAPI* was cloned into a pMAL-c2X expression vector after successful PCR amplification using the respective cloning oligomers (Table 1) designed with

Table 1
Oligomers used in this study.

Name	Purpose	Sequence (5′ →3′)
RbCIAPI_qF	BAC genomic library screening and qPCR amplification of *RbCIAPI*	GACTGGGTGCTCTCTTGCCT
RbCIAPI_qR	BAC genomic library screening and qPCR amplification of *RbCIAPI*	ACAACTTCAGAGCTGACATCAGCTTCT
RbCIAPI-F	ORF amplification (*Eco*RI)	GAGAGAgaattcATGGCAGACCTCGGCATCAA
RbCIAPI-R	ORF amplification (*Hin*dIII)	GAGAGAaagcttTCAAGCGTCCGTCAGCGT
Rb-βF	qPCR amplification of rock bream β-actin gene	TCATCACCATCGGCAATGAGAGGT
Rb-βR	qPCR amplification of rock bream β-actin gene	TGATGCTGTTGTAGGTGGTCTCGT

corresponding restriction sites *Eco*RI and *Hin*dIII. The PCR amplification was carried out in a TaKaRa thermal cycler using 50 μL of reaction mixture composed of 5 U of Ex*Taq* polymerase (TaKaRa, Japan), 5 μL of 10× Ex*Taq* buffer, 4 μL of 2.5 mM dNTPs, 80 ng of DNA template, and 20 pmol of each oligomer. The thermal cycling conditions were as follows: initial incubation at 94 °C for 30 s, 55 °C for 30 s, 72 °C for 1 min, and final extension at 72 °C for 5 min.

After cloning the respective PCR products, the resultant recombinant vector was transformed into *Escherichia coli* DH5α cells and confirmed by sequencing. Plasmids bearing the sequence confirmed *RbCIAPI* coding region were then transformed into *E. coli* BL21 (DE3) cells, and selected putative transformants were grown overnight in a 500 mL Luria–Bertani broth supplemented with 100 μg/mL ampicillin and 0.5 mg/mL glucose at 37 °C with shaking (200 rpm). After the optical density (OD) at 600 nm reached 0.6, isopropyl-β-thiogalactopyranoside (IPTG) was added at a final concentration of 1 mM and the mixture was incubated for 3 h at 37 °C to induce protein expression. Subsequently, cells were chilled on ice for 30 min and harvested by cold centrifugation. The obtained pellets were re-suspended in column buffer (20 mM Tris–HCl, pH 7.4, and 200 mM NaCl) and stored at –20 °C overnight. The following day, the cells were thawed under chilled conditions and ruptured by cold sonication in the presence of lysozyme (1 mg/mL). Thereafter, the resultant solution was separated by centrifugation (9000 × *g* for 30 min at 4 °C). The supernatant was defined as the crude extract and the recombinant protein was purified using the pMAL protein fusion and purification system (New England Biolabs, Ipswich, MA, USA). Subsequently, the concentration of the purified fusion protein product was determined using the Bradford method and integrity and purity were analyzed using 12% sodium dodecyl sulfate–polyacrylamide gel electrophoresis (SDS–PAGE) under reduced conditions.

2.3. Investigation of caspase inhibitory activity of RbCIAPI

In order to analyze the caspase inhibitory activity of RbCIAPI as a prominent evidence for its anti-apoptotic property, rRbCIAPI was used to inhibit the protease activity of recombinant rock bream mature caspase 3 (rRbcasp3) against its specific substrate DEVD-*p*NA. Briefly, rRbcasp3 was over expressed as a fusion protein with MBP similar to rRbCIAP and purified as described in our previous study (Elvitigala et al., 2012). Thereafter, four different amounts of purified rRbCIAPI (12.5 μg, 25 μg, 50 μg and 100 μg) were initially mixed with 50 μg of rRbcasp3 (achieving 4:1, 2:1, 1:1 and 1:2 rRbCIAPI:rRbcasp3 concentration ratios in the final solution) and incubated at 25 °C for 2 h in elution buffer (Column buffer + 10 mM maltose) (50 μL). Subsequently, the caspase 3 activity of rRbcasp3 in this mixture was investigated using a caspase 3 colorimetric activity assay kit (BioVision, USA), according to the manufacturer's instructions. Along with the experiments, rRbCasp3 (50 μg) or MBP (50 μg) was exclusively used as proteins in two separate control experiments. In another control experiment, recombinantly expressed and purified MBP (50 μg) using the same methodology was used in place of rRbCIAPI to determine the effect of MBP on the activity of rRbcasp3. Each assay was carried out in triplicate, and the mean OD_{405} values were determined for comparative analysis.

2.4. Animal rearing and tissue collection

Healthy rock bream fish with an average body weight of 50 g were selected for rearing from the Jeju Special Self-Governing province Ocean and Fisheries Research Institute (Jeju, Republic of Korea). The fish were reared under a controlled environment (salinity 34 ± 1‰, pH 7.6 ± 0.5) at 22–24 °C. All the animals were acclimatized for 1 week prior to the experimentation. Within the period of acclimatization, fish were fed with a commercially available fish feed. Whole blood (1 mL/fish) was collected from the caudal fin of three individuals using a sterilized syringe and the samples were immediately centrifuged at 3000 × *g* for 10 min at 4 °C to isolate the blood cells from the plasma. The collected cells were snap-frozen in liquid nitrogen. Meanwhile, the gills, liver, skin, spleen, head kidney, muscle, brain, heart, and intestine were excised from three sacrificed animals, which were immediately snap-frozen in liquid nitrogen and stored at –80 °C until used for total RNA extraction.

2.5. Immune stimulation studies

With the objective of investigating the modulatory properties of the rock bream iridovirus (RBIV), *Edwardsiella tarda*, lipopolysaccharides (LPS), and polyinosinic:polycytidylic acid (poly I:C) on *RbCIAPI* transcription, healthy rock breams were stimulated using aforementioned live pathogenic agents and pathogen-derived mitogens in time-course experiments, as described previously (Whang et al., 2011). *E. tarda* was obtained from the Department of Aqualife Medicine, Chonnam National University, Korea. The bacteria were incubated at 25 °C for 12 h in brain–heart infusion broth (Eiken Chemical Co., Japan) supplemented with 1% sodium chloride. The cultures were resuspended in sterile phosphate-buffered saline (PBS) and diluted to the desired concentration (1×10^5 CFU/mL) for injection. For the virus challenge experiment, kidney tissue specimens were obtained from moribund rock bream infected with RBIV and homogenized in 20 volumes of PBS. Tissue samples were centrifuged at 3000 × *g* for 10 min at 4 °C to obtain the RBIV containing supernatants. Supernatants were filtered through a 0.45 μm membrane and injected into the fish. LPS (1.25 μg/μL, *E. coli* 055:B5, Sigma) or poly I:C (1.5 μg/μL; Sigma) were resuspended in sterilized PBS for injection. Each animal was intraperitoneally (i.p.) injected with live *E. tarda* in PBS (5×10^3 CFU/μL) or 100 μL of LPS in PBS or 100 μL of poly I:C in PBS using sterilized syringes. Additionally, a control group was injected with an equal volume (100 μL) of PBS. Liver tissues of the experimental animals were collected as described in section 2.4 from three animals for each time period from each challenged group.

2.6. Total RNA extraction and reverse transcription

Total RNA was extracted from each of the excised tissues listed in section 2.4 from healthy fish and from liver tissues from the immune-challenged fish using Tri Reagent™ (Sigma-Aldrich; USA). The concentration of extracted RNA from different tissues was determined at 260 nm in a UV-spectrophotometer (Bio-Rad; USA) and diluted to 1 μg/μL. A portion (2.5 μg) of RNA from selected tissues was used to synthesize cDNA through reverse transcription using a cDNA synthesis kit (TaKaRa, Japan) according to the manufacturer's instructions. Finally, this newly synthesized cDNA was 40-fold diluted (total 800 μL) and stored at –20 °C until further analysis.

2.7. Determination of RbCIAPI transcript levels by quantitative real-time PCR (qPCR)

The transcript levels of *RbCIAPI* in the tissues listed in section 2.4 and the temporal expression of *RbCIAPI* in the liver of immune-challenged fish were investigated using the synthesized cDNA (section 2.6). After total RNA extraction followed by cDNA synthesis, qPCR was performed using the thermal cycler Dice™ Real time System (TP800, TaKaRa, Japan) in a 15-μL reaction volume containing 4 μL of diluted cDNA from corresponding tissues, 7.5 μL of 2× TaKaRa Ex Taq™ SYBR premix, 0.6 μL of each primer (RbCIAPI_qF and RbCIAPI_qR; Table 1), and 2.3 μL of ddH_2O, following the essential MIQE guidelines (Bustin et al., 2009). The qPCR was conducted

under the following conditions: 95 °C for 10 s, followed by 35 cycles of 95 °C for 5 s, 58 °C for 10 s, and 72 °C for 20 s; and a final cycle of 95 °C for 15 s, 60 °C for 30 s, and 95 °C for 15 s. The baseline was set automatically by Dice™ Real Time System software (version 2.00). *RbCIAPI* expression levels were determined by the Livak ($2^{-\Delta\Delta CT}$) method (Livak and Schmittgen, 2001). The same qPCR cycling profile was used for the internal reference gene, rock bream *β-actin* (GeneBank ID: FJ975146), using a corresponding pair of oligomers (Table 1). All data are represented as means ± standard deviation (SD) of relative mRNA expression (fold-change) of triplicates compared to expression of the rock bream *β-actin* gene. Moreover, the temporal expression fold-changes of *RbCIAPI* detected for the immune-challenged groups were normalized to the corresponding expression levels of phosphate-buffered saline (PBS)-injected controls, considering the effect of the medium of injection. To determine the statistical significance ($P < 0.05$) between the experimental and un-injected (0 h) control groups, a two-tailed unpaired Student's t-test was carried out.

3. Results and discussion

3.1. Sequence profile comparison and evolutionary position of RbCIAPI

The complete cDNA sequence of *RbCIAPI* was consisted of 1711 nucleotides including a 939 bp open reading frame (ORF), which encodes a protein of 313 amino acids (aa) with a predicted molecular mass of 33.25 kDa and a theoretical isoelectric point of 5.44, along with a 98 bp 5′ untranslated region (UTR) and a 674 bp 3′ UTR. The sequence information was deposited in the NCBI GenBank sequence database under the accession number KF408270. According to the online protein sequence analysis, RbCIAPI was found to bear a typical CIAPI domain architecture including the CIAPIN 1 domain and the signature of the *S*-adenosylmethionine-dependent methyltransferases superfamily (AdoMet) (Fig. 1). Pairwise sequence alignment of RbCIAPI with its homologs revealed that it shows substantial similarity and identity with its vertebrate counterparts, in which the most prominent similarity and identity values were shown with the CIAPI similitude of Atlantic salmon (85.9% and 74.1%, respectively; Table 2). Phylogenetic analysis of RbCIAPI clearly demonstrated its common ancestral origin of vertebrates, and further depicted its closer evolutionary relationship with fish counterparts (Fig. 2) based on the clustering pattern within the vertebrate clade. Moreover, the phylogenetic relationships further validated the prominent sequence homology of RbCIAPI with its counterpart of Atlantic salmon, detected in the pairwise sequence alignment study, forming a separate sub-cluster within the fish clade supported by a substantial bootstrapping value (74). However, CIAPI similitudes with fresh water telostan origin (zebrafish and catfish) grouped separately in the main fish clade with the support of maximum bootstrapping level (100). This clustering pattern demonstrates the distant evolutionary relationship of fresh water teleostan similitudes with those of marine teleosts (rock bream and salmon) included in the analysis.

According to the annotated genomic architecture of *RbCIAPI*, its complete genomic gene sequence was found to be split into 9 exons by 8 intronic sequences, in which the 5′ UTR is separated into two exons (Fig. 3). In order to gain insight into the genomic evolution of the *CIAPI* gene in vertebrate species, inter-species comparison of its genomic gene architecture was performed using several vertebrate counterparts obtained from the NCBI GenBank database (http://www.ncbi.nlm.nih.gov/gene), representing teleosts, amphibians, mammals, and birds as taxonomic levels (Fig. 3). This comparison revealed clear demarcation between the gDNA arrangements of teleostan origin and non-teleostan origin with respect to the sequence lengths of exons. In teleostan counterparts including *RbCIAPI*, sizes of the corresponding internal exons (exon 2 to exon 9) flanked by exonic sequences at the 3′ and 5′ ends were found to be almost perfectly conserved, except for slight deviations observed in the genomic gene arrangement of zebrafish (exons 6 and 7). Similarly, the sizes of corresponding internal exons were found to be almost completely conserved except exon 2 in non-teleostan similitudes. Nevertheless, as a common feature shared by all counterparts considered in the comparison, the 5′ UTR was split into two exons, even though their sizes were observed to be different. Moreover, it is worth noting that the exon number is conserved among all of the vertebrate genes included in the comparison, demonstrating no gain or loss of introns throughout the genomic evolutionary process of *CIAPIs* from lower vertebrate lineages (teleosts) to higher vertebrate lineages (mammals). Hence, the overall outcome of the comparison further revealed that molecular evolution of vertebrate CIAPI counterparts has occurred at a relatively slow rate, as demonstrated through the insignificant size differences of most of the exons among the different species. In addition, a multi-exonic genomic architecture of *CIAPIs* was observed, even in the lower vertebrate lineages such as teleosts. This observation suggests the potential proteomic diversity of vertebrate CIAPIs through post-transcriptional modification mechanisms such as alternative splicing and exon shuffling, which certainly merits further investigation (Keren et al., 2010).

3.2. Tissue-specific expression pattern of RbCIAPI

According to the qPCR analysis, ubiquitous transcription of *RbCIAPI* was detected in tissues examined, albeit at different magnitudes (Fig. 4). Highly prominent transcription of *RbCIAPI* was observed in the blood cells and liver tissues, whereas lower, but considerable mRNA expression levels were detected in the heart and brain tissues. Interestingly, Rbcasp3 also exhibited the same pattern of spatial distribution, as reported in our previous study (Elvitigala et al., 2012). This suggests a close functional relationship between RbCIAPI and Rbcasp3 in rock bream physiology, since CIAPIs are known to inhibit the apoptotic process of cells via obstructing caspase activity (Luo et al., 2012).

The blood and liver are known to bear immune cells such as phagocytes, promoting their indispensible function in the host defense system. Upon exposure to the pathogenic invaders, these cells can evoke potent anti-microbial activities including the generation of ROS (DeLeo, 2004). Therefore, cells in the blood and liver tissues are prominently active in metabolism. However, this hyperactivity along with potent excessive ROS production can trigger the frequent apoptosis of these cells (Simon et al., 2000). Thus, the regulatory mechanisms of apoptosis, in terms of inhibition, should also be activated to prevent excessive apoptosis in the blood and liver cells, which may explain our observation of strong expression levels of CIAPI in the rock bream liver and blood tissues. Moreover, the liver is known to be involved in detoxification processes in animals; hence susceptible to many toxic agents internalized in the body. Therefore, hepatocytes will undergo frequent apoptosis, which should be regulated to maintain a positive physiological status. Thus, it is not surprising to observe abundant expression of anti-apoptotic molecules such as CIAPIs in liver tissues of animals, including fish species.

Previous reports can also account for the universally distributed expression pattern of CIAPI among different tissues in different taxonomic groups. For instance, human CIAPI was detected consistently in almost all of the tissue types examined in both the adult and fetal stages, where high levels of expression were encountered in the heart, muscle, and digestive tract in both fetal and adult tissues. Moreover, fetal stage tissues also showed prominent expression of CIAPI in the liver and skin (Hao et al., 2006). CIAPI expression in fetal rat tissues demonstrated a more diverse pattern,

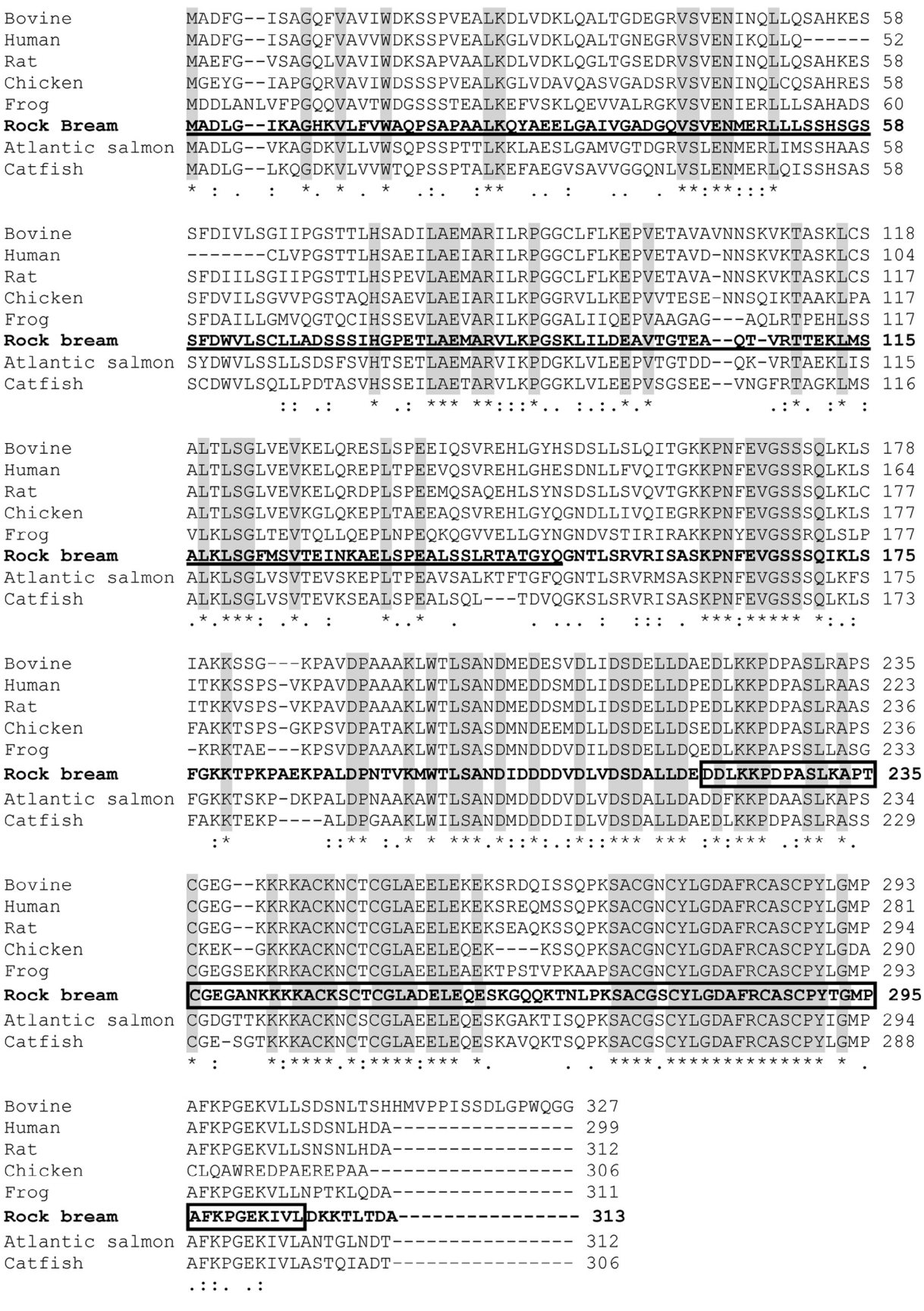

Fig. 1. Multiple sequence alignment of RbCIAPI with its vertebrate counterparts. Sequence alignments were conducted using the ClustalW method. Conserved residues among all the sequences are shaded in gray, whereas the *in silico*-predicted CIAPIN-1 domain and AdoMet signature are boxed and underlined, respectively.

Table 2
Percent similarity and identity values of RbCIAPI with its orthologs.

Name of the species	NCBI-GenBank accession number	Amino acids	Similarity (%)	Identity (%)
1. *Salmo salar* (Atlantic salmon)	ACH70653	312	85.9	74.1
2. *Ictalurus punctatus* (catfish)	NP001188008	306	79.3	69.7
3. *Danio rerio* (zebrafish)	CAM14258	341	72.9	60.6
4. *Heterocephalus glaber* (rat)	EHB00656	312	71.4	54.6
5. *Homo sapiens* (human)	EAW82923	299	70.2	53.7
6. *Crotalus adamanteus* (viper)	AFJ49438	306	70.1	53.2
7. *Xenopus laevis* (frog)	NP001164545	311	68.9	53.1
8. *Bos taurus* (bovine)	AAI20106	327	68.1	53.0
9.*Gallus gallus* (chicken)	NP001005834	306	67.3	51.4
10. *Acromyrmex echinatior* (ant)	EGI61280	283	52.8	38.4
11. *Lepeophtheirus salmonis* (salmon louse)	ACO12287	292	49.6	35.2

in which adult rat brain and spinal cord tissues showed greater expression than other tissues of the body, whereas expression levels were lower in the small intestine, muscle, and kidney tissues (Park et al., 2011).

3.3. *Transcriptional response of* RbCIAPI *against pathogenic stress*

To anticipate the potential inhibitory regulation of RbCIAPI on apoptosis upon pathogen invasion, its temporal transcriptional modulation under pathogenic stress was analyzed in liver tissues using qPCR. As depicted in Fig. 5A, LPS stimulation triggered a repressive transcriptional response at the early phase (3 h post stimulation [p.s.]) of the experiment, and then elicited induction of transcription at subsequent time points (12 h and 24 h p.s.), compared to the basal transcription levels. However, transcript levels were downregulated again at 48 h p.s., reflecting a complex modulatory pattern. On the other hand, the live bacterial pathogen *E. tarda* positively regulated *RbCIAPI* expression continuously from 6 h to 48 h p.s. Intriguingly, in our previous investigation, the same immune stimuli elicited an inductive transcriptional response of *Rbcasp3*, a key mediator of apoptosis (Elvitigala et al., 2012). Therein, LPS could also upregulate *Rbcasp3* expression at 12 h and 24 h p.s., whereas *E. tarda* could evoke continuous transcriptional upregulation throughout the whole experimental period.

Some bacteria are known to induce apoptosis as a method of propagating infection according to their virulence (Lancellotti et al., 2006). Moreover, cell surface receptors such as toll-like receptors can identify LPS-like pathogen-associated molecular patterns (PAMPs) of bacteria, which triggers signaling pathways that ultimately induce apoptosis of the cells (Bannerman and Goldblum, 2003). Therefore, a potential host defense mechanism against this process of pathogenesis probably involves in induction of the expression of anti-apoptotic molecules in host cells, herein immune cells in liver such as macrophages like phagocytes (Castro et al., 2014). The observed elevations in *RbCIAPI* and *Rbcasp3* expression upon LPS and *E. tarda* stimulation can be associated with this explanation, since CIAPI can potentially play a significant role in obstruction of apoptosis. On the other hand, as mentioned in the previous section, ROS production is a key first line host immune response which mounts against a pathogen invasion. Fish liver tissues are known to harbor phagocytes such as macrophages and other hepatic leukocytes like dendritic cells (Castro et al., 2014) which potentially produce ROS against different stimuli including pathogen sensing (Dupré-Crochet et al., 2013). However, surpluses of ROS can also trigger oxidative stress and in turn apoptotic cell death (Circu and Aw, 2010). Thus, it is not illogical to expect that expression of anti-apoptotic molecules like CIAPIs are induced to counterbalance the death of aforementioned immune cells in liver tissues. However, the detected downregulated expression levels in response to LPS stimulation at the early and late phases of the experiment may have been caused by failure of the mechanisms discussed earlier, resulting in the induction of apoptosis. Collectively, the detected prominent and prolonged upregulated temporal transcriptional profile of *RbCIAPI* upon bacterial stimulation compared to LPS stimulation may reflect the potent ability of live pathogenic stimulants to trigger a rapid and effective immune response in host cells than its PAMPs (Mourao-Sa et al., 2013).

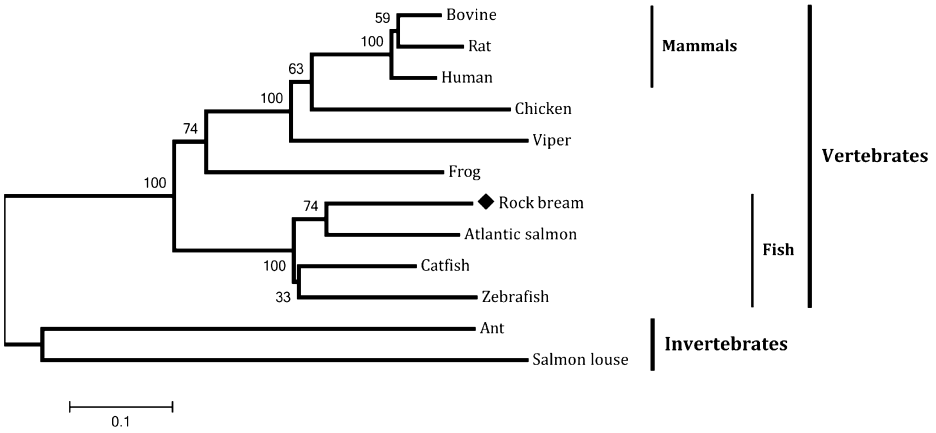

Fig. 2. Phylogenetic reconstruction of RbCIAPI. Evolutionary relationship of RbCIAP with different CIAPI counterparts was determined based on alignments of respective protein sequences using the neighbor-joining method of MEGA 4.0 software. Corresponding bootstrap support for each branch is indicated on the tree diagram. NCBI GenBank accession numbers of the CIAPI members represented on the tree are listed in Table 2.

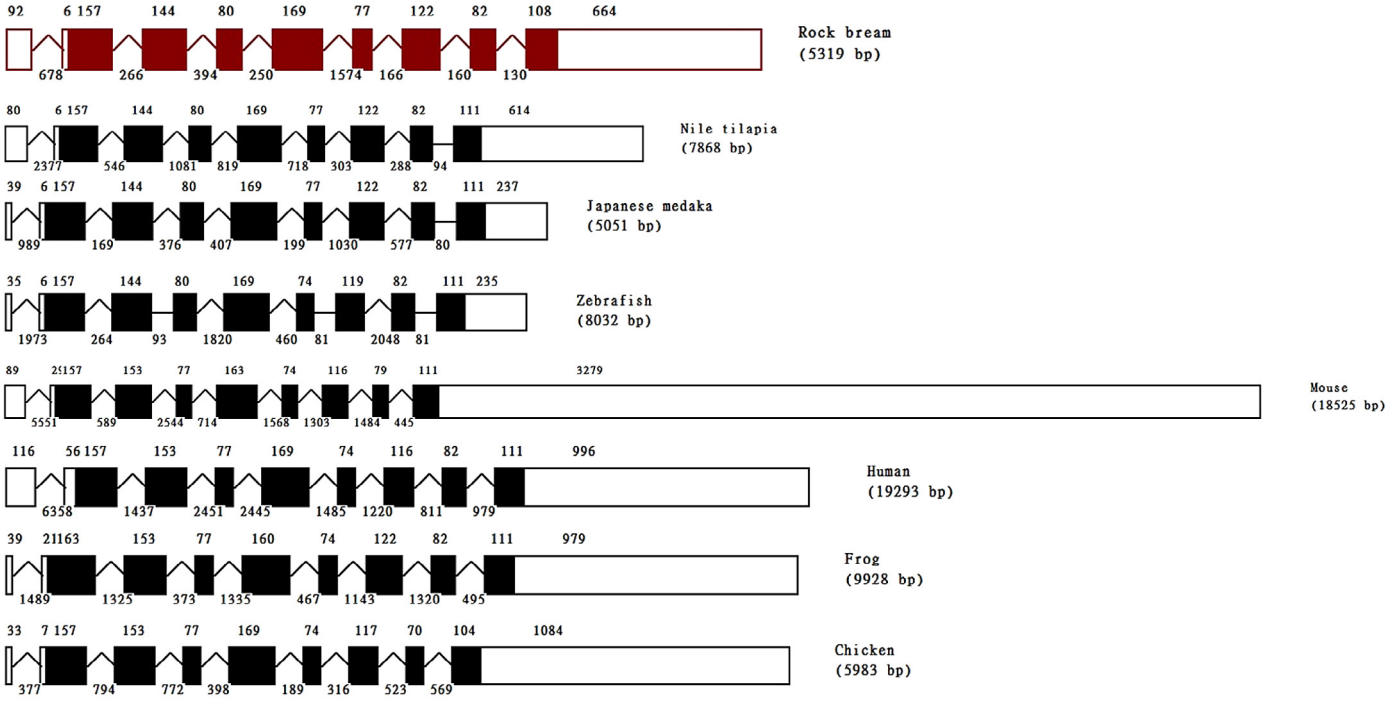

Fig. 3. Exon–intron arrangement along the genomic *RbCIAPI* gene and comparison with its vertebrate counterparts. Empty boxes represent the UTR regions of the exons, whereas the color-filled boxes represent coding regions. Introns less than 100 bp are denoted with black lines and others (>100 bp) are depicted using Λ-shaped symbols. The corresponding DNA sequence lengths of introns and exons are indicated at the top and bottom of each structure, respectively. The genomic DNA sequence information of each counterpart was obtained from the NCBI GenBank database under the following gene IDs: Nile tilapia – 100712254, Japanese Medaka – 101167114, Zebrafish – 445283, Mouse – 109006, Human – 57019, Frog – 100490633, and Chicken – 41563. (For interpretation of the references to color in this figure legend, the reader is referred to the web version of this article.)

As depicted in Fig. 5B, live RBIV exposure induced the expression of *RbCIAPI* at the middle and late phases of the experiment, whereas the viral dsRNA emulator poly I:C suppressed its transcription at the middle phase after stimulation. As a host defense mechanism, apoptosis is known to become activated in viral-infected cells after recognition of the infected agents, most likely through recognition of their PAMPs by the corresponding immune sensors (Hardwick, 2001). In order to facilitate this, host defense

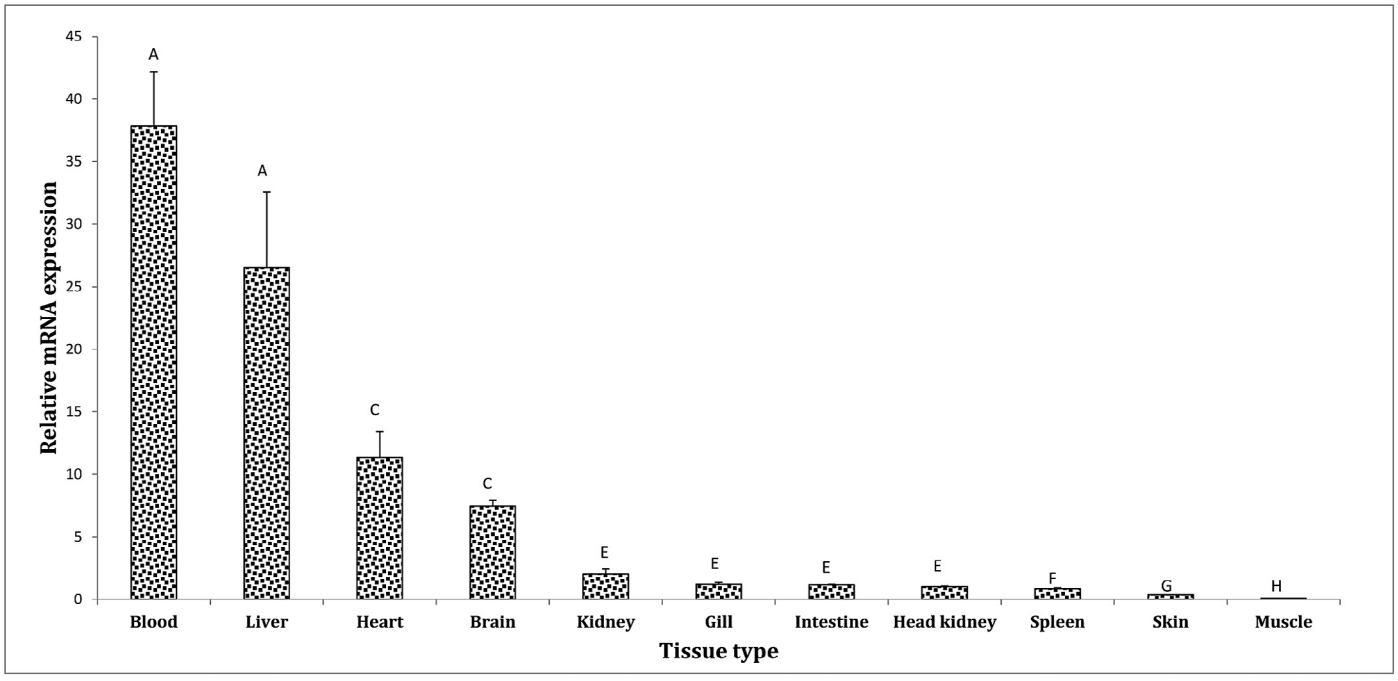

Fig. 4. Specific distribution of *RbCIAPI* determined by qPCR. Expression fold-difference of each tissue was determined compared to the expression level of the head kidney. Error bars represent the SD (n = 3). Bars labeled with different letters represent significantly different ($p < 0.05$) expression levels.

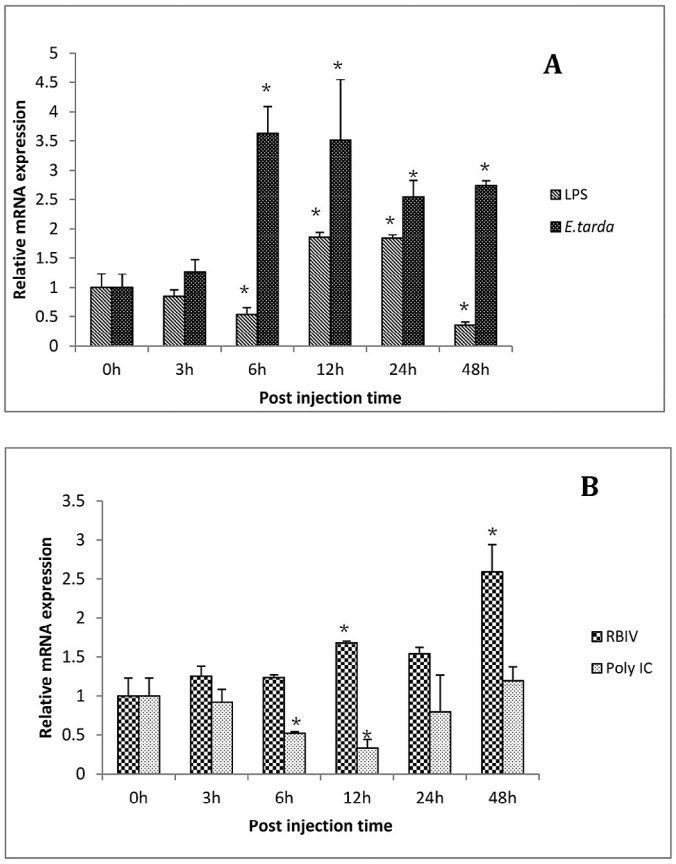

Fig. 5. Transcriptional modulation of *RbCIAPI* upon exposure to pathogen stress in rock bream liver tissue, generated by (A) *E. tarda* and LPS, and (B) poly I:C and RBIV, as determined by qPCR. The relative expression levels were calculated by the $2^{-\Delta\Delta CT}$ method, using rock bream *β-actin* as a reference gene, further normalizing to the corresponding expression levels of PBS-injected controls at each time point. The relative expression fold-change at 0 h post-stimulation (un-injected control) was used as the basal value. Error bars represent the SD (n = 3); $^{*}p < 0.05$.

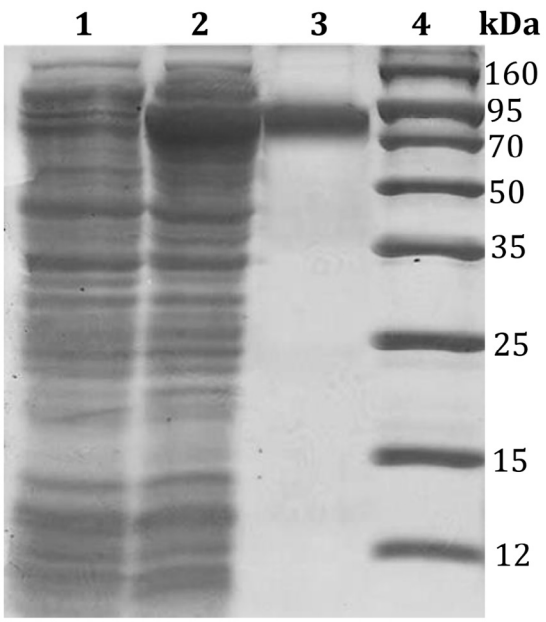

Fig. 6. SDS–PAGE analysis of the overexpressed and purified recombinant RbCIAPI fusion protein; lane 1, total cellular extract from *E. coli* BL21 (DE3) harboring the rRbCIAPI-MBP expression vector prior to IPTG induction; lane 2, crude extract of rRbCIAPI fusion protein; lane 3, purified recombinant fusion protein (rRbCIAPI-MBP); lane 4, protein size marker (Enzynomics; Korea).

mechanisms may potentially suppress the expression of anti-apoptotic molecules, including CIAPI in infected cells. Our observation of an under-expressed transcriptional profile after exposure to poly I:C may reflect this hypothesis, which is further supported by our previously reported expression modulation of *Rbcasp3* in response to the same stimulus, where transcriptional elevations of *Rbcasp3* were observed at the middle phase of the experiment (Elvitigala et al., 2012).

On the other hand, viruses have previously been shown to inhibit the apoptosis of infected host cells as an evasion mechanism of host anti-viral defense (Brien, 1998). Therefore, it is not illogical to suggest that the detected induction of *RbCIAPI* expression upon the invasion of RBIV in liver tissues also may be triggered by the live virus against the host immune defense to obstruct the apoptosis prompted against the infection in cells such as macrophages and phagocytic leukocytes (Castro et al., 2014). This suggestion can be further validated based on our previously reported inductive response of *Rbcasp3* to the same stimulus at the late phase of the experiment, which reflects the potential elicitation of apoptosis against the viral infection as a host immune response (Elvitigala et al., 2012).

3.4. Integrity and purity of rRbCIAPI

SDS–PAGE analysis of the different components obtained from the rRbCIAPI expression and purification procedure demonstrated the successful overexpression of our target rRbCIAPI fusion protein product by IPTG induction under the experimental conditions, further revealing the substantial purity and integrity of the ultimately obtained eluted protein product (Fig. 6). The protein band corresponding to the purified rRbCIAPI fusion protein indicated a molecular mass of ~76 kDa, showing compatibility with the predicted molecular mass of RbCIAPI (33.25 kDa), since the molecular mass of MBP is known to be ~42.5 kDa.

3.5. In vitro *caspase inhibitory activity of rRbCIAPI*

In order to decipher the potential anti-apoptotic property of RbCIAPI possibly through inhibition of caspase activity, caspase3 inhibitory activity of rRbCIAP was evaluated using rRbCasp3 as the target. As detected, pre-incubation of rRbcasp3 with three different amounts (25 μg, 50 μg and 100 μg) of rRbCIAPI notably inhibited the proteases activity of Rbcasp3 against its specific substrate DEVD-*p*NA, reflected by a significantly low ($P < 0.01$) OD_{405} values (0.84, 0.59 and 0.67, respectively) compared to the control reaction (1.82), in which exclusively rRbcasp3 was used as a protein (Fig. 7). Also we could detect a dose dependent inhibitory activity of rRbCIAPI in the comparison of 25 μg and 50 μg treated assays, although there was no significant OD difference ($P < 0.01$) noted between 50 μg and 100 μg of rRbCIAPI treated assays. Almost similar OD values resulted in doublings the treated concentrations of final two experiments hints the optimum concentration ratio between rRbcasp3 and RbCIAPI is 1:1 in activity inhibition. As expected, MBP alone did not show any protease activity against DEVD-*p*NA and the activity of rRbCasp3 incubated with MBP in place of rRbCIAPI in control experiments was not affected, evidencing the negligible interference of MBP tag and any potential bacterial factors exist in each recombinant fusion protein on their respective functional properties. Collectively, our observations in this experimental approach suggest that the putative anti-apoptotic properties of RbCIAPI are likely exerted through the functional inhibition of a caspase-dependent

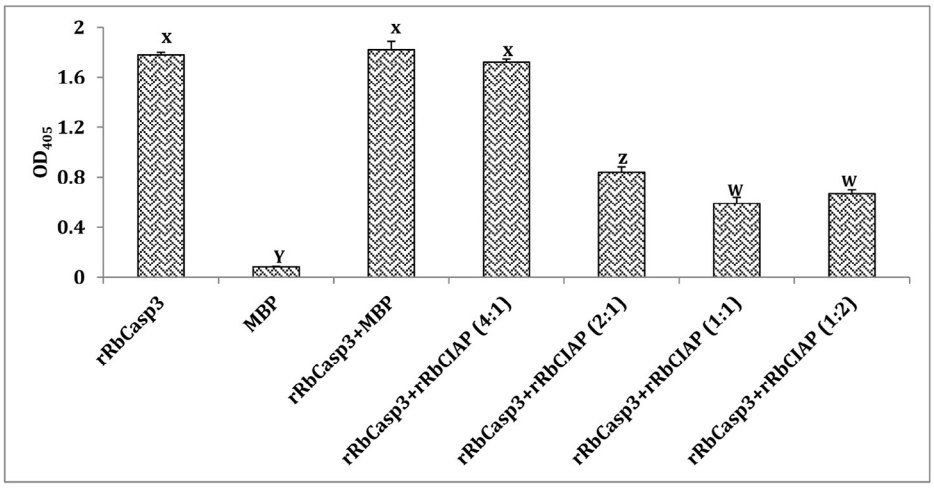

Fig. 7. Effect of rRbCIAPI on protease activity of rRbcasp3 against DEVD-*p*NA. X axis shows corresponding assays. Error bars represent SDs (n = 3). Significantly different ($P < 0.05$) OD_{405} values are represented by different letters.

apoptosis process in rock bream. Supporting our observations, a previous study reported that caspase 3 activity of schistosome lysates was inhibited by CIAPI, more or less similar manner to our observations, with different concentrations of its recombinant protein, suggesting the potent inhibitory function of CIAPI from *Schistosoma japonicum* on caspases in schistosomes *in vitro* (Luo et al., 2012).

4. Conclusion

RbCIAPI consisted of a typical CIAPI domain architecture, which was confirmed by sequence analysis. Furthermore, phylogenetic analysis revealed its orthology and close evolutionary relationship with CIAPI counterparts of other fish species. *RbCIAPI* showed multi-exonic genomic gene architecture, intimating the possibility of the existence of spliced isoforms. Moreover, our qPCR results confirmed that *RbCIAP* shows ubiquitous specific expression, and its transcriptional modulation under pathogenic stress was further demonstrated. In addition, RbCIAPI demonstrated detectable *in-vitro* caspase inhibitory activity by suppressing the protease activity of Rbcasp3. Collectively, these findings suggest that RbCIAPI may act as a regulator of caspase-dependent apoptosis by inhibiting Rbcasp3 activity and its expression can be modulated by pathogen infections.

Acknowledgment

This research was supported by the project titled 'Development of Fish Vaccines and Human Resource Training', funded by the Ministry of Oceans and Fisheries, Korea and by the National Fisheries Research and Development Institute (RP-2015-BT-003) grant.

References

Bannerman, D.D., Goldblum, S.E., 2003. Mechanisms of bacterial lipopolysaccharide-induced endothelial apoptosis. Am. J. Physiol. Lung Cell. Mol. Physiol. 284, 899–914.
Brien, V.O., 1998. Viruses and apoptosis. J. Gen. Virol. 79, 1833–1845.
Burlacu, A., 2003. Regulation of apoptosis by Bcl-2 family proteins. J. Cell. Mol. Med. 7, 249–257.
Bustin, S.A., Benes, V., Garson, J.A., Hellemans, J., Huggett, J., Kubista, M., et al., 2009. The MIQE guidelines: minimum information for publication of quantitative real-time PCR experiments. Clin. Chem. 55, 611–622. doi:10.1373/clinchem.2008.112797.
Castro, R., Abós, B., Pignatelli, J., Jørgensen von Gersdorff, L., González Granja, A., Buchmann, K., et al., 2014. Early immune responses in rainbow trout liver upon viral hemorrhagic septicemia virus (VHSV) infection. PLoS ONE 9, 1–13.
Circu, M.L., Aw, T., 2010. Reactive oxygen species, cellular redox systems, and apoptosis. Free Radic. Biol. Med. 48, 749–762.
Danial, N.N., Korsmeyer, S.J., 2004. Cell death: critical control points. Cell 116, 205–219.
DeLeo, F.R., 2004. Modulation of phagocyte apoptosis by bacterial pathogens. Apoptosis 9, 399–413. doi:10.1023/B:APPT.0000031448.64969.fa.
Deveraux, Q.L., Reed, J.C., 1999. IAP family proteins — suppressors of apoptosis IAP family proteins – suppressors of apoptosis 239–252.
Dupré-Crochet, S., Erard, M., Nüβe, O., 2013. ROS production in phagocytes: why, when, and where? J. Leukoc. Biol. 94, 657–670.
Elmore, S., 2007. Apoptosis: a review of programmed cell death. Toxicol. Pathol. 35, 495–516. doi:10.1080/01926230701320337.
Elvitigala, D.A.S., Whang, I., Premachandra, H.K.A., Umasuthan, N., Oh, M.-J., Jung, S.-J., et al., 2012. Caspase 3 from rock bream (Oplegnathus fasciatus): genomic characterization and transcriptional profiling upon bacterial and viral inductions. Fish Shellfish Immunol. 33, 99–110.
Everett, H., McFadden, G., 1999. Apoptosis: an innate immune response to virus infection. Trends Microbiol. 7, 160–165.
Gastric, M., Cells, C., 2006. CIAPIN1 confers multidrug resistance by upregulating the expression ND ES RIB. Cancer Biol. Ther. 5, 261–266.
Hao, Z., Li, X., Qiao, T., Zhang, J., Shao, X., Fan, D., 2006. Distribution of CIAPIN1 in normal fetal and adult human tissues. J. Histochem. Cytochem. 54, 417–426. doi:10.1369/jhc.5A6753.2005.
Hardwick, J.M., 2001. Apoptosis in viral pathogenesis. Cell Death Differ. 8, 109–110. doi:10.1038/sj.cdd.4400820.
Keren, H., Lev-Maor, G., Ast, G., 2010. Alternative splicing and evolution: diversification, exon definition and function. Nat. Rev. Genet. 11, 345–355.
Lancellotti, M., Brocchi, M., Dias, W., 2006. Bacteria-induced apoptosis: an approach to bacterial pathogenesis. Braz. J. Morphol. Sci. 23, 75–86.
Li, X., Hong, L., Zhao, Y., Jin, H., Fan, R., Du, R., et al., 2007. A new apoptosis inhibitor, CIAPIN1 (cytokine- induced apoptosis inhibitor 1), mediates multidrug resistance in leukemia cells by regulating MDR-1, Bcl-2, and Bax. Biochem. Cell Biol. 1, 741–750. doi:10.1139/O07-141.
Li, X., Pan, Y., Fan, R., Jin, H., Han, S., Liu, J., et al., 2008. Adenovirus-delivered CIAPIN1 small interfering RNA inhibits HCC growth in vitro and in vivo. Carcinogenesis 29, 1587–1593. doi:10.1093/carcin/bgn052.
Livak, K.J., Schmittgen, T.D., 2001. Analysis of relative gene expression data using real-time quantitative PCR and the 2(–Delta Delta C(T)) method. Methods 25, 402–408. doi:10.1006/meth.2001.1262.
Luo, R., Zhou, C., Shi, Y., Zhao, J., Cheng, G., 2012. Molecular characterization of a cytokine-induced apoptosis inhibitor from *Schistosoma japonicum*. Parasitol. Res. 111, 2317–2324. doi:10.1007/s00436-012-3086-4.
Mourao-Sa, D., Roy, S., Blande, J.M., 2013. Vital-PAMPS: signatures of microbial viability. In: Katsikis, P.D., Schoenberger, S.P., Pulendran, B. (Eds.), Crossroads Between Innate and Adaptive Immunity IV. Springer, New York, pp. 1–136.
Park, K.-A., Yun, N., Shin, D.-I., Choi, S.Y., Kim, H., Kim, W.-K., et al., 2011. Nuclear translocation of anamorsin during drug-induced dopaminergic neurodegeneration in culture and in rat brain. J. Neural Transm. 118, 433–444. doi:10.1007/s00702-010-0490-8.
Shibayama, H., Takai, E., Matsumura, I., Kouno, M., Morii, E., Kitamura, Y., et al., 2004. Identification of a cytokine-induced antiapoptotic molecule anamorsin essential for definitive hematopoiesis. J. Exp. Med. 199, 581–592. doi:10.1084/jem.20031858.

Shizusawa, T., Shibayama, H., Murata, S., Saitoh, Y., Sugimoto, Y., Matsumura, I., et al., 2008. The expression of anamorsin in diffuse large B cell lymphoma: possible prognostic biomarker for low IPI patients. Leuk. Lymphoma 49, 113–121. doi:10.1080/10428190701713697.

Simon, H.U., Haj-Yehia, A., Levi-Schaffer, F., 2000. Role of reactive oxygen species (ROS) in apoptosis induction. Apoptosis 5, 415–418.

Sun, E.W., Shi, Y.F., 2001. Apoptosis: the quiet death silences the immune system. Pharmacol. Ther. 92, 135–145.

Tamura, K., Dudley, J., Nei, M., Kumar, S., 2007. MEGA4: Molecular Evolutionary Genetics Analysis (MEGA) software version 4.0. Mol. Biol. Evol. 24, 1596–1599. doi:10.1093/molbev/msm092.

Whang, I., Lee, Y., Lee, S., Oh, M.-J., Jung, S.-J., Choi, C.Y., et al., 2011. Characterization and expression analysis of a goose-type lysozyme from the rock bream *Oplegnathus fasciatus*, and antimicrobial activity of its recombinant protein. Fish Shellfish Immunol. 30, 532–542. doi:10.1016/j.fsi.2010.11.025.